Flocculation of Clay Suspensions by Anionic and Cationic Polyelectrolytes: A Systematic Analysis

Ahmad Shakeel [1,2,*], Zeinab Safar [1], Maria Ibanez [1,†], Leon van Paassen [3], and Claire Chassagne [1]

[1] Department of Hydraulic Engineering, Faculty of Civil Engineering and Geosciences, Delft University of Technology, Stevinweg 1, 2628 CN Delft, the Netherlands; Z.Safar-1@tudelft.nl (Z.S.); Maria.IbanezSanz@anteagroup.com (M.I.); C.Chassagne@tudelft.nl (C.C.)

[2] Department of Chemical, Polymer & Composite Materials Engineering, University of Engineering & Technology, KSK Campus, Lahore 54890, Pakistan

[3] School of Sustainable Engineering and the Built Environment, Arizona State University, 650 E Tyler Mall, 85287-3005, Tempe, Arizona, USA; leon.vanpaassen@asu.edu

* Correspondence: a.shakeel@tudelft.nl

† Current address: Antea Group, 2600 Antwerpen, Belgium.

Received: 13 October 2020; Accepted: 5 November 2020; Published: 10 November 2020

1. Experimental

1.1. Rheological Measurements

The rheological properties of pure clay suspensions (no added flocculant) were analysed using a HAAKE MARS I rheometer (Thermo Scientific, Germany) with concentric cylinder (Couette) geometry. Before each experiment, a waiting time of 3–5 minutes was used, in order to eliminate the disturbances created by the Couette geometry. In order to analyse the wall slip phenomenon during measurement, which is quite common in these kinds of suspensions [1], Couette geometry with a grooved surface was also used. The results are similar for both smooth and grooved Couette geometries, which showed the absence of wall slip (data not shown). The rheological experiments were performed at different concentrations of clay ranging from 110 to 1000 g/L (i.e., from 10 to 50 wt%), which were high enough to have interactions between the particles, in order to assess the rheological fingerprint of the suspensions. Each experiment was carried out in duplicate to check the repeatability of the measurements and that the measurement error was less than 2%. The following rheological tests were performed to analyse the pure clay samples:

1.1.1. Stress Ramp-Up Test

Stress ramp-up tests were performed using the stress-controlled mode of the rheometer. An increasing stress was applied from 0 to 100 Pa at a rate of 1 Pa/s. The corresponding torque was measured, and the shear rate and viscosity were then determined.

1.1.2. Frequency Sweep Test

Preliminary amplitude sweep tests were carried out at a constant frequency of 1 Hz to estimate the linear viscoelastic (LVE) regimes. Frequency sweep tests were then performed from 0.1 to 100 Hz within the linear viscoelastic regime. The storage modulus (G') and loss modulus (G'') were recorded as a function of frequency.

1.1.3. Structural Recovery Test

The structural recovery test was started with a waiting time of 100 s (i.e., oscillatory time sweep within LVE), after reaching the measurement position, to eliminate the disturbances created by the geometry and also to estimate the storage modulus before the structural breakup. The steady shearing step was then performed at a shear rate of 300 s^{-1} for the duration of 500 s. After that,

structural recovery was carried out by performing oscillatory time sweep experiments within the linear viscoelastic regime at the frequency of 1 Hz for 500 s.

2. Results and Discussion

2.1. Clay Suspensions Without Flocculant

2.1.1. Rheological Analysis

The rheological analysis of clay suspensions in the absence of flocculant was performed. The clay concentration was varied from 10 to 50 wt% (110 to 1000 g/L) in order to analyse the effect of concentration on the rheological impression. Stress ramp-up tests were performed to estimate the yield stresses of our clay suspensions due to their wide applicability for yield stress analysis. Figure S1a shows the results of stress ramp-up tests for different clay suspensions. It is visible from the figure that the suspensions at lower concentrations (i.e., 10–20 wt%) behave like a shear-thinning liquid with no yield stress, while at higher concentrations (i.e., 25 and 30 wt%), the suspensions display a viscosity plateau followed by a viscosity decline due to the presence of a yield stress (i.e., formation of clay clusters). At even higher concentrations (40 and 50 wt%), the results show two distinct viscosity declines (i.e., two-step yielding phenomenon). The two yield stresses are estimated from the sharp declines in viscosity by an extrapolation method [2]. The stress values corresponding to the first decline were defined in previous studies [3,4] as "static yield stress", τ_y^s, and linked with the breakage of the (isotropic) slurry structure into mobile clusters of particles. The positioning of these clusters with the flow leads to shear thinning, as there is less resistance to flow. The second decline was termed as "fluidic yield stress", τ_y^f, and was attributed to the breakage of the clusters into smaller clusters or individual particles [3,4]. Note that this behaviour is in contrast with the behaviour reported by [5], where shear thickening is expected after a shear-thinning phase upon an increase in the shear rate. In the case of shear-thickening, the formation of so-called hydroclusters is observed [6]. The single decline in clay suspensions at intermediate concentrations (i.e., 25 and 30 wt%) was also termed fluidic yield stress as the clay particles, even at low shears, are expected to be able to flow in clusters (in contrast to higher clay concentrations, there is no shear threshold for the formation of these clusters). A similar dependence of two-step yielding on the solids concentration was also reported in the literature for hard sphere suspensions [7,8]. It was observed that the two-step yielding process converged into a single-step yielding below the solids volume fraction of 0.2.

In order to determine the linear viscoelastic regime, preliminary oscillatory amplitude sweep tests at a constant frequency were performed. The frequency sweep tests were then carried out within the linear viscoelastic regime to examine the mechanical properties of the suspensions without affecting their structure. The outcome of frequency sweep tests is shown in Figure S1b,c in terms of the complex modulus and phase angle as a function of frequency, for different clay suspensions. It was observed that the complex modulus of the suspensions with lower concentrations, particularly 10 wt%, displayed a strong frequency dependency along with a cross-over ($\delta = 45°$) in the phase angle behaviour, which confirmed their liquid-like character. However, the suspensions at higher concentrations (i.e., above 20 wt%) behave as a solid-like material with a weak dependency of the complex modulus on frequency and small phase angle values with no cross-over. At higher frequencies, an increase in the complex modulus and a decrease in phase angle values was evident, which was due to the rheometer head inertial effects. These experimental data, at higher frequencies, were removed from the figures to eliminate the misconception. A similar solid-like behaviour of natural sediments as a function of frequency, within the linear viscoelastic regime, was previously reported in the literature [9–11]. Figure S1d shows the fluidic yield stress values and complex modulus values at 1 Hz as a function of weight fraction of clay. Both parameters displayed an exponential increase with the increase in clay content (i.e., linear increase in semi-log scale); however, the complex modulus displayed a stronger dependency on clay content as compared to the fluidic yield stress. The similar exponential increase in yield stresses and moduli as a function of

density/solids volume fraction was also reported in the literature for different mud sediments [12–14].

Structural recovery experiments were also performed for the unflocculated clay suspensions, in order to analyse the structural re-growth in the clay suspensions after the shearing action. A simple model adapted from [15] was used to interpret the data of storage modulus as a function of time after pre-shearing, given as follows:

$$\frac{G'}{G'_0} = \frac{G'_i}{G'_0} + \left(\left(\frac{G'_\infty - G'_i}{G'_0}\right)\left(1 - \exp\left[-\left(\frac{t}{t_r}\right)^d\right]\right)\right) \quad (1)$$

where G' is the time dependent storage modulus of clay suspensions after pre-shearing, G'_0 is the storage modulus before shearing, G'_i is the storage modulus right after shearing action (i.e., G' at t→0) and G'_∞ is the time invariant storage modulus as time approaches infinity; t_r is the characteristic time of the material and represents the rate of structural build-up; and d is the stretching exponent which mirrors the sensitivity of storage modulus on time and its value usually lies within the range of 0-1. The fitting parameters in Equation (1) are the following: G'_∞, t_r and d.

The results of structural recovery tests in terms of normalized storage modulus (with respect to the initial storage modulus value) as a function of time, after the pre-shearing step, are shown in Figure S2 for different clay suspensions. The structural re-growth was not studied for the suspensions with clay concentrations less than 30 wt% due to the settling behavior at such lower concentrations. It can be seen from the results that suspensions with higher clay content display lower recovery of structure. However, the suspensions with low clay content, in particular 30 wt%, display a comparatively high structural recovery, which may be linked to the disapearance of individual clay clusters after breakup (restructuring of the clay matrix). This higher recovery in structure may also be linked to the settling of particles at such low concentration. An opposite behavior, i.e., increase in structural recovery with the increase in solids volume fraction, was observed for the iron oxide suspensions in mineral oil [16], which may be due to the absence of two-step yielding in those suspensions. The values of the rheological parameters for the investigated suspensions are listed in Table S1.

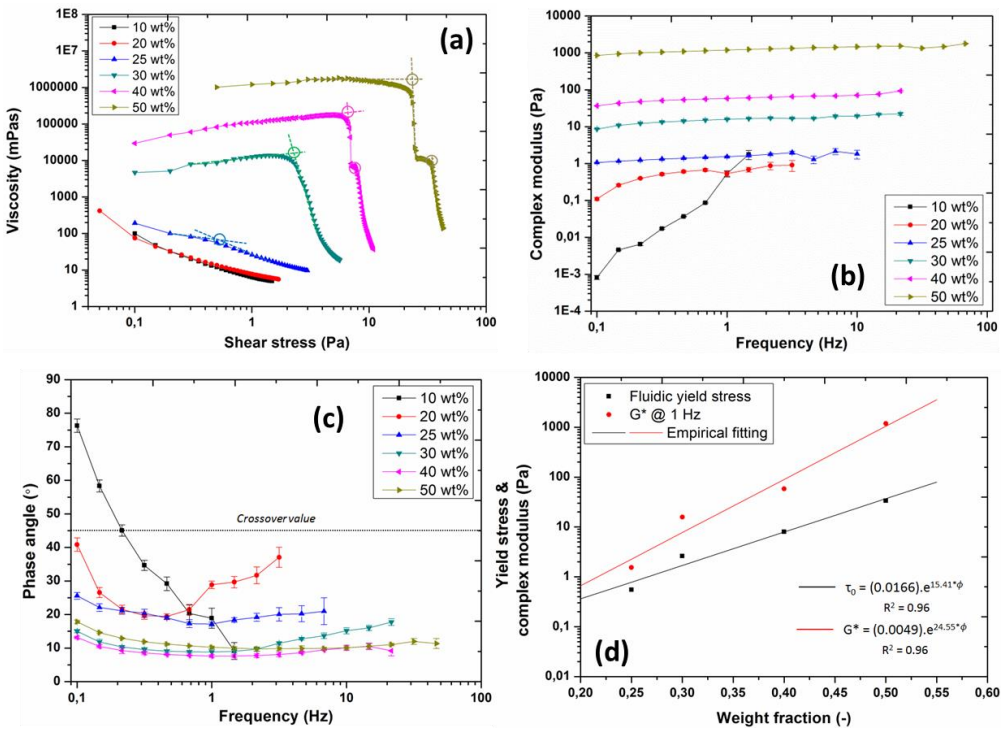

Figure S1. (**a**) Apparent viscosity as a function of stress; (**b**) complex modulus and (**c**) phase angle as a function of frequency, bars represent the standard deviation; (**d**) fluidic yield stress and complex modulus values at 1 Hz as a function of weight fraction of clay, solid lines represent the empirical fitting.

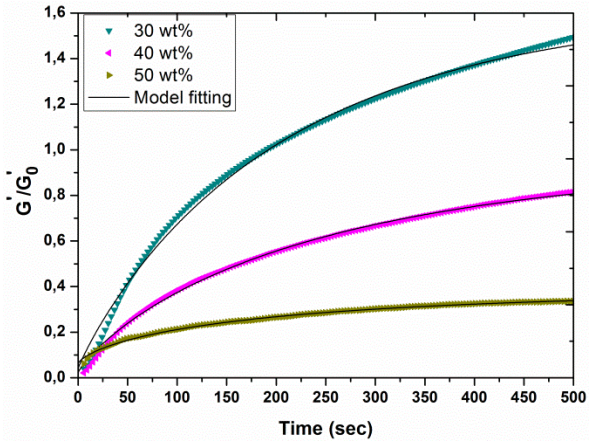

Figure S2. Normalized storage modulus as a function of time, after the pre-shearing step, for different clay suspensions, solid lines represent the empirical model fitting.

Table S1. The values of the rheological parameters for the investigated clay suspensions.

Weight %	Static Yield Stress (Pa)	Fluidic Yield Stress (Pa)	G* at 1 Hz (Pa)	δ at 1 Hz (°)	t_r (sec)	G'_∞ (Pa)	G'_∞/G'_0	d (-)
25	-	0.55	1.54	17	-	-	-	-
30	-	2.6	15.81	9	209	21.65	1.64	0.92
40	6.3	8	58.36	8	244	55.52	0.96	0.84
50	22	33.5	1190.63	9	198	409.52	0.39	0.70

2.1.2. Settling Rate

Two preliminary settling studies were also performed on pure clay suspensions (with no added flocculant). The clay concentration was 50 and 70 g/L. It was possible to fit the data corresponding to the free settling of clay particles, i.e., the water/suspended particles interface h as function of time t, using Richardson and Zaki's formulation [17]:

$$h(t) = h_0 - v_{Stokes} \cdot (1 - \phi_s/\phi_{gel})^m \cdot t \quad (2)$$

where m is an empirical fit coefficient which usually varies between 3 and 6 [18], $h_0 = h(t = 0)$ is the initial height, v_{Stokes} is Stokes settling velocity, ϕ_s is the solid volume fraction and ϕ_{gel} is the volume fraction at gelling (i.e., when particles are forming an interconnected network). We used $\phi_{gel} = 0.74$ (volume fraction for random packing of hard spheres) as an estimate. This gelling volume fraction corresponds to a fluid density of $\phi_{gel} \times 2600 + (1 - \phi_{gel}) \times 1000 = 2184\ g/L$, where we took the absolute density of clay to be 2600 g/L and the absolute density of water to be 1000 g/L. From Figure S3, it can be seen that Stokes formulation ($m = 0$) already predicts quite well the settling phase until 800 s after the start of the experiment. After 800 s, the measured data start to deviate from Stokes formulation and a coefficient $m = 5$ was found to best fit the data. Above 6000 s, the last clay particles are deposited on the clay bed, and from that time on, the water–clay bed interface can be followed in time. This occurs at the so-called gel time. This part of the data will not be discussed in the present paper which concentrates on clay suspensions, and we refer to [19] for further discussion on the consolidation of clay beds.

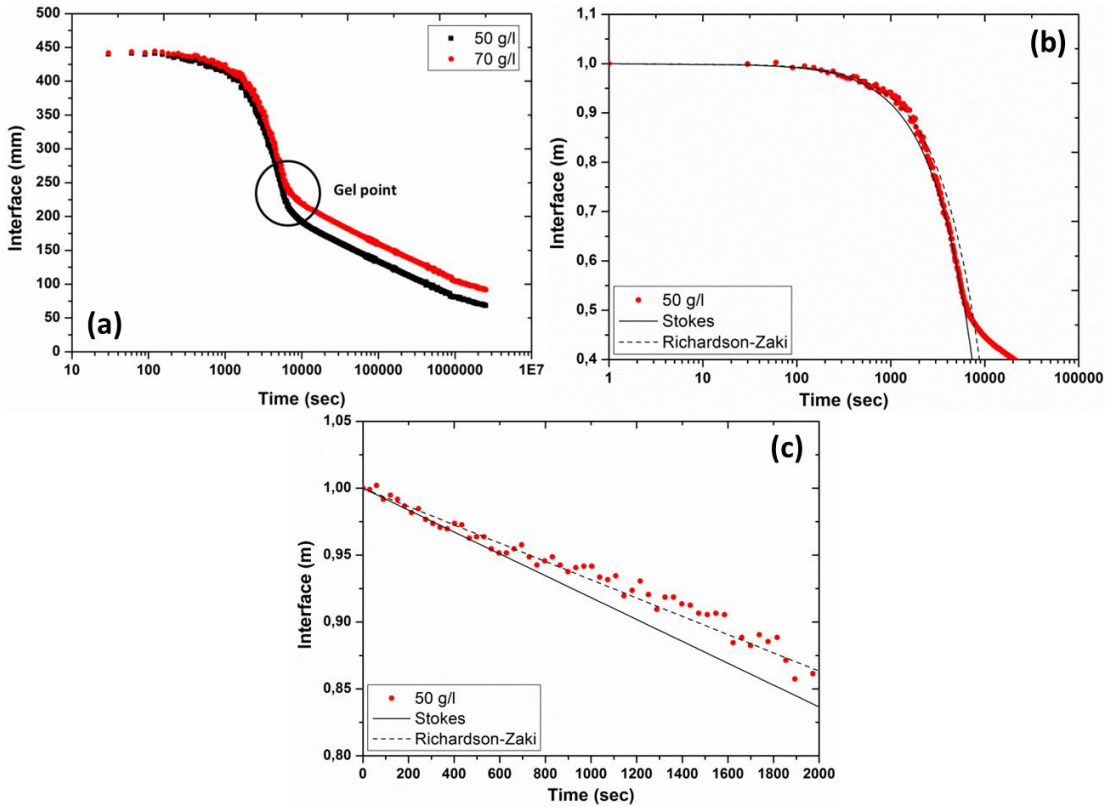

Figure S3. Water–suspended clay interface as a function of time. (**a**) The settling behaviour of clay at two different clay concentrations, (**b**) and (**c**) examples of fitting the data for the 50 g/l sample using either the Stokes formulation ($m = 0$) or the Richardson-Zaki formulation with $m = 5$, see Equation (2). The height has been normalized (h/h_0 has been plotted) in (b) and (c).

References

1. Barnes, H.A. A review of the slip (wall depletion) of polymer solutions, emulsions and particle suspensions in viscometers: its cause, character, and cure. *J Nonnewton Fluid Mech* **1995**, *56*, 221–251.
2. Zhu, L.; Sun, N.; Papadopoulos, K.; Kee, D.D. A slotted plate device for measuring static yield stress. *J Rheol.* **2001**, *45*, 1105–1122.
3. Shakeel, A.; Kirichek, A.; Chassagne, C. Rheological analysis of mud from Port of Hamburg, Germany. *J. Soils Sediments.* **2020**, *20*, 2553–2562.
4. Shakeel, A.; Kirichek, A.; Chassagne, C. Is density enough to predict the rheology of natural sediments? *Geo-Marine Letters* **2019**, *39*, 427–434.
5. Mewis, J.; Wagner, N.J. *Colloidal suspension rheology*; Cambridge University Press: 2012.
6. Maranzano, B.J.; Wagner, N.J. The effects of interparticle interactions and particle size on reversible shear thickening: Hard-sphere colloidal dispersions. *J Rheol.* **2001**, *45*, 1205–1222.
7. Koumakis, N.; Petekidis, G. Two step yielding in attractive colloids: transition from gels to attractive glasses. *Soft Matter* **2011**, *7*, 2456–2470.
8. Kramb, R.C.; Zukoski, C.F. Yielding in dense suspensions: cage, bond, and rotational confinements. *J. Phys. Condens. Matter.* **2010**, *23*, 035102.
9. Xu, J.; Huhe, A. Rheological study of mudflows at Lianyungang in China. *Int. J. Sediment Res.* **2016**, *31*, 71–78.
10. Soltanpour, M.; Samsami, F. A comparative study on the rheology and wave dissipation of kaolinite and natural Hendijan Coast mud, the Persian Gulf. *Ocean Dyn.* **2011**, *61*, 295–309.

11. Van Kessel, T.; Blom, C. Rheology of cohesive sediments: comparison between a natural and an artificial mud. *J. Hydraul. Res.* **1998**, *36*, 591–612.
12. Huang, Z.; Aode, H. A laboratory study of rheological properties of mudflows in Hangzhou Bay, China. *Int. J. Sediment Res.* **2009**, *24*, 410–424.
13. Fass, R.W.; Wartel, S.I. Rheological properties of sediment suspensions from Eckernforde and Kieler Forde Bays, Western Baltic Sea. *Int. J. Sediment Res.* **2006**, *21*, 24–41.
14. O'Brien, J.S.; Julien, P.Y. Laboratory analysis of mudflow properties. *J. Hydraul. Eng.* **1988**, *114*, 877–887.
15. Mobuchon, C.; Carreau, P.J.; Heuzey, M.-C. Structural analysis of non-aqueous layered silicate suspensions subjected to shear flow. *J Rheol.* **2009**, *53*, 1025–1048.
16. Kanai, H.; Navarrete, R.C.; Macosko, C.W.; Scriven, L.E. Fragile networks and rheology of concentrated suspensions. *Rheol. Acta.* **1992**, *31*, 333–344.
17. Richardson, J.F.; Zaki, W.N. The sedimentation of a suspension of uniform spheres under conditions of viscous flow. *Chem. Eng. Sci.* **1954**, *3*, 65–73.
18. Dhont, J.K.G. *An introduction to dynamics of colloids*; Elsevier: Oxford, United Kingdom, 1996.
19. Chassagne, C. Understanding the natural consolidation of slurries using colloid science In Proceedings of European Conference on Soil Mechanics and Geotechnical Engineering, Reykjavik, Iceland, 1–7 September 2019.